J Mater Sci (2008) 43:4753–4759
DOI 10.1007/s10853-008-2665-3

Electrodeposition of lead zirconate titanate nanotubes

A. Nourmohammadi · M. A. Bahrevar · S. Schulze · M. Hietschold

Received: 4 October 2007 / Accepted: 18 April 2008 / Published online: 3 June 2008

Abstract Lead zirconate titanate (PZT) nanotubes have been grown using porous anodic alumina templates. Sol–gel electrophoretic deposition method was utilized to form the nanotubes on pore walls. The templates were prepared using various anodizing voltages to achieve different pore diameters. Phosphoric acid solution was employed as the electrolyte. Stabilized PZT sols were prepared using lead acetate trihydrate and modified precursors of zirconium and titanium with acetic acid. The filled templates were then sintered at 700 °C. Scanning electron microscopy (SEM) shows that tubular PZT arrays have been efficiently grown in the alumina templates. Transmission electron microscopy (TEM) further confirms the tubular form and polycrystalline nature of the tubes. Energy dispersive X-ray (EDX) analyses also confirm the composition of the tubes. X-ray diffraction (XRD) spectra indicate the presence of the perovskite PZT as the main phase.

A. Nourmohammadi · S. Schulze · M. Hietschold
Solid Surfaces Analysis and Electron Microscopy Group, Institute of Physics, Chemnitz University of Technology, 09107 Chemnitz, Germany
e-mail: abolghasem.nourmohammadi@physik.tu-chemnitz.de

S. Schulze
e-mail: schulze@physik.tu-chemnitz.de

M. Hietschold
e-mail: hietschold@physik.tu-chemnitz.de

A. Nourmohammadi · M. A. Bahrevar (✉)
Semiconductors Department, Materials and Energy Research Center (MERC), 31779-83634 Karaj, Iran
e-mail: ma-bahrevar@merc.ac.ir; ma.bahrevar@yahoo.com

Introduction

In recent years, research on inorganic nanotubes such as metals, semiconductors, or oxides has been rapidly increasing. Ferroelectric oxide nanotubes are suitable one-dimensional structures for many functional nanodevices such as nanoscale sensors and actuators and nanoelectromechanical systems (NEMS) because the sensitivity and efficiency of such devices are directly proportional to the surface area of the material. Therefore, much effort has already been devoted to develop various ferroelectric oxide nanotubes [1–4].

Lead zirconate titanate or PZT, with the perovskite structure, is a well known ferroelectric and piezoelectric ceramic material with high spontaneous polarization, dielectric permittivity, and piezoelectric coefficients. With the general formula of $Pb(Zr_xTi_{1-x})O_3$, $0 < x < 1$, it is a binary solid solution of $PbZrO_3$, an antiferroelectric with orthorhombic structure, and $PbTiO_3$, a ferroelectric with tetragonal perovskite structure. PZT refers to the whole compositional range of this solid solution which includes various amounts of tetragonal and rhombohedral phases below the Curie point. However, the dielectric permittivity and piezoelectric coefficients of PZT ceramics generally peak at compositions near the so-called morphotropic phase boundary or MPB. This boundary occurs at $x = 0.52$ and is nearly temperature independent [5].

It has been acknowledged that the template-based synthesis process is a very useful technique for the production of various one-dimensional nanostructures including nanorods, nanowires, and nanotubes [6]. In this process, a liquid or gaseous precursor of the desired material is deposited into some porous structure, such as porous anodic alumina (AA) membranes, mesoporous silicone, or polycarbonates. However, the ferroelectric materials grown

in this manner are amorphous and should be annealed to recrystallize into the desired ferroelectric phase. When amorphous PZT compositions are annealed to form the perovskite phase, an intermediate fluorite (or pyrochlore) phase is first crystallized [7]. The presence of this non-ferroelectric phase, even in small amounts, causes deterioration of the electrical properties of the whole system. Therefore, it is necessary to minimize or, if possible, totally avoid the formation of this phase.

The template-wetting process is known as the main method in the production of PZT nanotubes [8]. A solid layer containing lead, zirconium, and titanium precursors is formed in this deposition method on the pore walls of the template. This layer is then annealed to crystallize into the perovskite phase in a tubular form. A polymer-based solution is normally prepared in this method by addition of a suitable polymer material to the PZT sol in order to decrease the surface energy and increase the wetting of the pore walls with the solution. This increases both the organic content of the solid layer and the shrinkage of the tubes during firing which, in turn, can potentially lead to cracks and defects in the tubular structure due to the large volume contraction. It seems that post-annealing of the tubes after template removal is necessary to reduce these defects and release the residual stress [1–2]. Therefore, it is strongly desirable to use an alternative method more compatible with low carbon content PZT gels in order to decrease the shrinkage upon firing.

It is well known in sol–gel processing that surface-charged nanoclusters with the desired stochiometry are generated by hydrolysis and condensation reactions during sol preparation. This surface charge interacts with other charged species in the sol to produce a double-layer charged structure around the particle. Electrostatic stabilization of the sol is based on this charged structure which prevents agglomeration. Sol–gel electrophoretic deposition is based on the application of an external electric field to such an electrostatically stabilized sol. The externally applied electric field forces these charged particles to move toward the electrodes inserted in the sol and, therefore, could be used for the deposition of the particles on the electrode. This method is used for the production of thin and thick films and yields films of greater thickness, density, and quality than the traditional sol–gel method alone [9]. In addition, it has been widely utilized to produce nanorods or nanowires of metallic materials and alloys [10–14] as well as nanorods of both simple and complex oxides [15–17].

In the present work, sol–gel electrophoretic deposition is used to produce PZT nanotube arrays. Porous AA membranes are produced to form the nanotubes using a template-based method. Stabilized PZT sols with near MPB composition are used to form nanotubes with low carbon content in order to minimize the shrinkage upon firing. The aim of this work is to obtain PZT tubular arrays with the perovskite structure and avoid the formation of the undesired non-ferroelectric phases in the process.

Experimental procedure

The first step of this research is to prepare the porous alumina templates through a two-step anodizing process using commercially available aluminum foils (0.2 mm thick). The Al foils were first cleaned and annealed in nitrogen ambient at 500 °C for 3 h to increase the grain size and provide better homogeneity for the development of the pores. The foil surfaces were then polished using three electropolishing steps in a mixture of 4:4:2 by weight of H_3PO_4, H_2SO_4, and H_2O [18]. During the electrochemical polishing, a constant electropolishing current of $\sim$2 A/cm^2 was used for 40 s intervals. The electropolishing solution was cooled down intermittently to avoid the extra heating of the solution due to high currents. The polished aluminum sheets were anodized in a 10 wt.% aqueous solution of phosphoric acid to obtain a nanoporous aluminum oxide layer on the surface. A cooled electrochemical cell, held constant at 1 °C, was used for anodizing. The first anodized layer was subsequently removed in a mixture of phosphoric acid (6 wt.%) and chromic acid (1.8 wt.%) at 60 °C [19]. Both the first and the second anodizing processes were carried out under the same voltages in the range of 45–114 V to control the pore diameters in the 80–200 nm range, and the second anodizing step was done over different periods of time from 11 to 24 h to obtain pore lengths varying from about 8 to 30 μm. After anodizing, the unanodized aluminum substrate was removed in a saturated solution of $HgCl_2$ and the barrier layer of the prepared templates were opened and the pores were simultaneously broadened after etching in a 5 wt.% phosphoric acid solution for about 4 h at room temperature. Figure 1 shows a typical SEM planar view of a porous AA template, prepared as described. The template has been anodized at 80 V and the average pore diameter is $\sim$140 nm. Figure 2 shows the cross-sectional view of the same template as in Fig. 1 with the pores widened. Some of the pores have branched, but a rather uniform and parallel array of the channels has been achieved after pore broadening. It is also clear that the average pore diameter has increased to $\sim$230 nm.

Lead zirconate titanate sols with the composition of $Pb_{1.1}(Zr_{0.52}Ti_{0.48})O_3$ were prepared using lead acetate trihydrate (99.999%, Aldrich), zirconium (IV) butoxide (80% in *n*-butanol, Aldrich), and titanium (IV) butoxide (97%, Aldrich) as the precursors and glacial acetic acid (100%, Assay, Karl Roth) as the modifier. Excess lead acetate

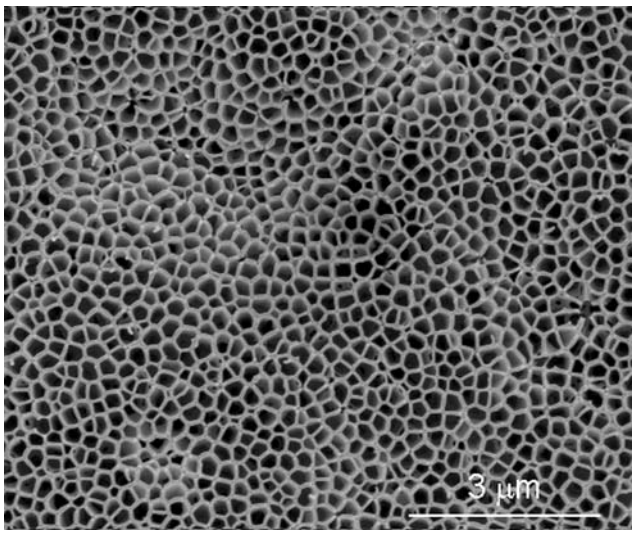

Fig. 1 An SEM plan view of a porous AA template, anodized at 80 V

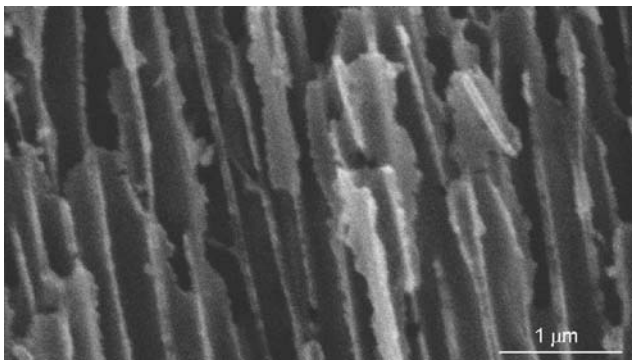

Fig. 2 Fracture view of an AA template, after pore broadening

(10 mol.%) was also added to compensate for the lead loss during the firing process. Lead acetate trihydrate (20.86 g) was first dissolved in glacial acetic acid (24.2 mL) ultrasonically. The prepared solution was dehydrated at 110 °C for 15 min and then cooled down to room temperature. Zirconium (IV) butoxide (11.9 mL) was also mixed ultrasonically with titanium (IV) butoxide (8.4 mL) for several minutes. In order to prepare a useable sol, the zirconium butoxide/titanium butoxide mixture was first mixed with the lead acetate/acetic acid solution at room temperature to chemically change the hydrolysis behavior of these materials with acetic acid. Lead acetate/acetic acid solution was dehydrated first because water could cause non-uniform gelation of zirconium and titanium butoxides, before they were modified. Deionized water (0.1 μS/cm, 3.6 mL) was subsequently added to the prepared solution to hydrolyze the zirconium and titanium precursors. The hydrolyzed precursor solution was diluted with 44.6 mL methanol (100%, Fisher Scientific) to prevent fast gelation of the sol. Ethylene glycol (99.5%, 3.1 mL), glycerol (99.5%, 4.14 mL), and lactic acid (90 wt.%, 2.9 mL) were also added to enhance viscosity and stability of the final solution [20, 21]. The prepared solution was magnetically stirred and stored in sealed containers. The resulting sol was transparent and stable for at least 8 weeks.

DC electrophoretic deposition process was used to fill the template channels with the prepared PZT sol. The bottom of the templates was first coated by sputtering a 100-nm thick gold film to produce the so-called working electrode. The coated template was fixed in a specifically designed stainless steel holder to be connected to an external power supply during the deposition process. A platinum mesh was also used as the counter electrode. Due to the hygroscopic nature of the used precursor materials, an inert (N_2) atmosphere was used during the deposition. The entire process was carried out at room temperature. The filled templates were dried at 100 °C for 12 h, and then fired at 700 °C for 1 h in air to develop the desired perovskite structure.

X-ray diffraction (XRD) analyses were carried out on the fired templates with a Philips PW-3710 diffractometer, using Cu–Kα radiation. Scanning electron microscopy (SEM) was used on etched templates with both a Leica/Cambridge S360 and an FEI Nano Nova 200 SEM system. An energy dispersive X-ray (EDX) spectrometer was also used to analyze the composition of the grown nanotubes. Transmission electron microscopy (TEM) was employed to investigate the thinned templates using a Philips CM-200 FEG-HRTEM system.

Results and discussion

Scanning electron microscopy

Figure 3 shows the SEM planar view of an array of the grown PZT nanotubes. This array of nanotubes has been prepared by heavy etching of the template in a 40 wt.% caustic soda solution at room temperature. The filled template, after etching, has been rinsed with deionized water and subsequently dried. It is clearly evident that the electrophoretic deposition of the prepared sol has resulted in a hollow tubular structure. The average outer diameter of the tubes is about 230 nm which is consistent with the broadened pores of the template in Fig. 2. Although the template shown in Fig. 3 has been heavily etched, the separating walls between the tubes, in some areas, can be distinguished.

Figure 4 shows a larger area of the same sample as in Fig. 3 at a lower magnification. It is observed that nearly all of the channels are filled and the grown PZT array has covered the whole visible area of the template which shows good filling efficiency of the porous alumina template with

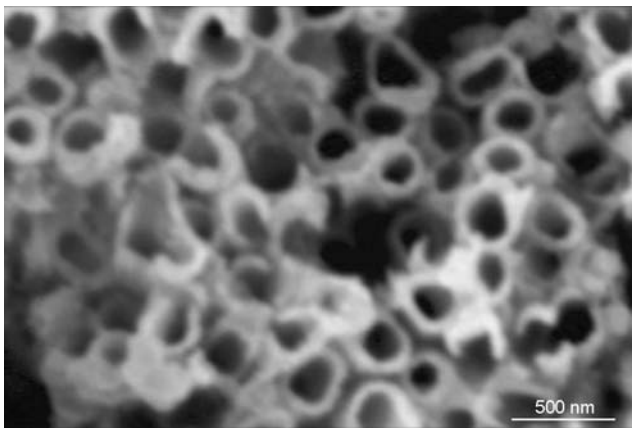

Fig. 3 SEM micrograph of an array of PZT nanotubes, sticking out of the template after etching

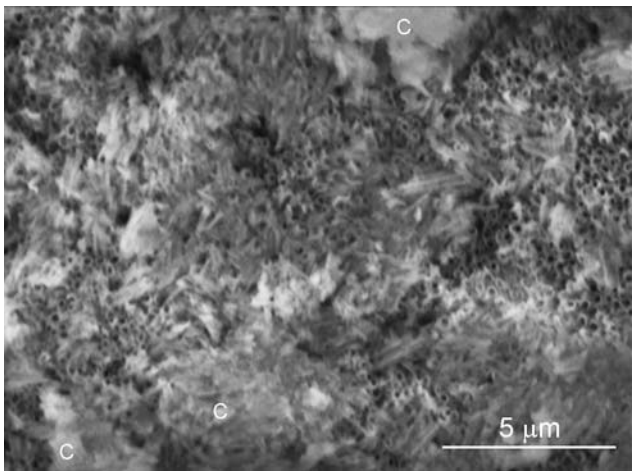

Fig. 4 SEM micrograph of the etched template in Fig. 3 at lower magnification

the PZT nanotubes. The hollow nature of the array in the figure indicates that a tubular rather a rod or wire-like structure is formed throughout. However, two technical problems are observed in this figure: first, the nanotubes are covered with a PZT surface deposit in certain areas and second, the tubes do not have a uniform height after template removal. The surface deposit is marked by the letter "C" in some areas in Fig. 4. It is frequently observed in the template-based sol deposition of nanostructures and is a common problem in the production of PZT nanotubes by template-wetting method [1]. This feature is also observed in sol electrophoretic deposition of the nanorods of both simple and complex oxides [15–17] and is due to mechanical removal of excess sol from the surface.

Both of the above-mentioned problems can be avoided if the surface of the sample is slightly milled with argon ion beam. Figure 5 shows the SEM image of another array of the electrophoretically grown nanotubes. This array was deposited at the electrophoretic voltage of 1.2 V for 30 min

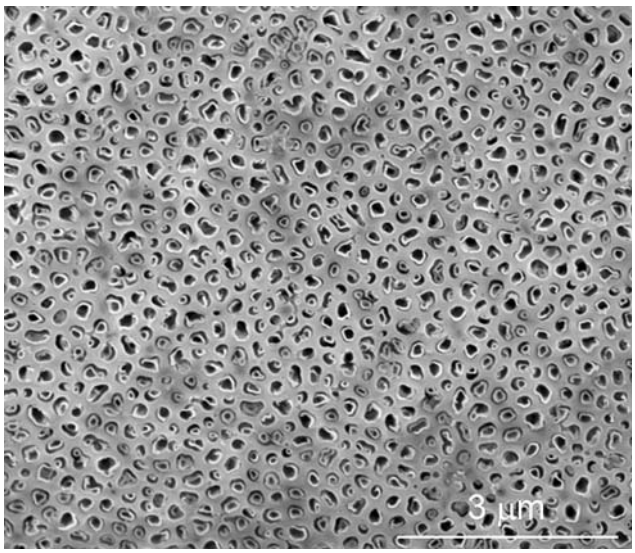

Fig. 5 SEM micrograph of a filled porous alumina template after slight ion-milling and partial etching

and the average outer diameter of the tubes is about 200 nm. The filled template in this image, after firing, has been ion-milled by a Bal Tec RES 100 ion-beam device for 30 min and then partially etched in a 5 wt.% caustic soda solution at room temperature. It is observed that the template contains a flat and uniform array of parallel nanotubes. Both Figs. 4 and 5 show that nearly all of the channels are filled with the PZT nanotubes which indicate the suitability of the DC electrophoretic deposition technique as an effective method for filling the empty channels of the AA templates.

Transmission electron microscopy

Transmission electron microscopy was utilized to investigate both the form and crystallinity of the grown nanotubes. Figure 6 shows a bright-field TEM image of the grown nanotubes. The porous alumina template is also visible in the micrograph as the matrix. The alumina membrane and one of the tubes are marked in this image by the letters "A" and "T", respectively. To prepare this sample, the filled alumina membrane was thinned by ion-beam milling for about 10 h and then slightly etched in a 5 wt.% caustic soda solution at room temperature. The grown tubes have subsequently stuck out of the milled template after etching.

It is observed that the two channels at the top of the image (Fig. 6a) are empty whereas the others contain some nanotubes. An empty pore is marked in this image by the letter "P". Since the template is heavily thinned, it is easy for some of the tubes at the edges to disentangle from the supporting template after etching. Therefore, we expect that the tubes which belong to the empty channels have

Fig. 6 Bright-field TEM images of (**a**) empty and filled pores of an AA membrane and (**b**) a tube wall. Electron diffraction patterns of (**c**) the alumina matrix and (**d**) tube wall in (**b**)

already left their positions. It is easy to measure the diameter of the empty pores now, but the measured size of the hollow channels is not representative of the real diameter of the grown tubes, because they are excessively broadened during etching. Pore broadening is observed in the filled pores of Fig. 6a too. Fig. 6b also shows a bright-field TEM image of an AA channel with the PZT nanotube, sticking out of the template after etching. Part of the tube wall is observed in this image without any hindrance.

Crystallinity of the template matrix and the tube wall was investigated by electron diffraction and the relevant images are shown in Fig. 6c and d, respectively. The first image shows that the matrix is amorphous, as expected, whereas diffraction image of the tube wall indicates the polycrystalline nature of the tube.

EDX analysis

Energy dispersive X-ray (EDX) analyses were carried out to evaluate the composition of the tubes qualitatively. Figure 7 shows the EDX spectrum of the nanotube array of Fig. 3. The sample was mounted on a glass substrate using epoxy resin; therefore, the spectrum represents the X-ray lines from the array of the nanotubes as well as the carbon line originating mainly from the epoxy resin. The aluminum line is from the porous alumina template, and the sodium line is due to the residues of caustic soda used for etching of the template. Since platinum has been used to coat the sample, platinum lines are also observed. Taking these considerations into account, we can conclude that the analyzed nanotubes, grown in an AA template, are composed of titanium, zirconium, and lead oxides.

Formation of nanotubes

The prepared PZT sol was driven into the template channels under the influence of various DC electrophoretic voltages of 0.8–4.8 V over different periods of time up to 90 min. At higher voltages (>4 V), however, major fluctuations in the electrical current were observed and instability set in. In fact, no deposition took place at these voltages, and microscopic evaluation of the templates did not reveal any tubes.

In constant-voltage electrophoresis, the potential between the electrodes is maintained constant, hence, with increasing deposition (and therefore, increasing electrical resistance), the electrophoretic current decreases; so does

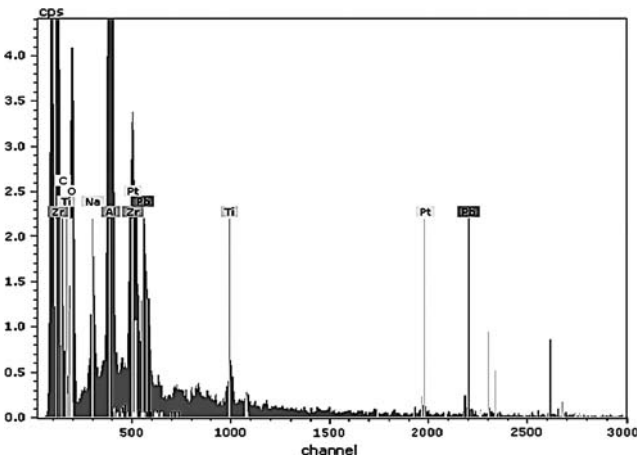

Fig. 7 EDX spectrum of an array of the grown nanotubes

the deposition rate [22]. A typical plot of the total electrophoretic current versus time for the deposition of the PZT nanotubes is presented in Fig. 8. Similar behavior of the electrophoretic current versus time was also observed at greater deposition times. It must be noted that the above behavior has been observed at low voltages.

The use of template-based electrophoretic deposition in the growth of nanowires and rods of complex oxides has already been discussed [9, 15–17]. Successful growth of nanotubes of complex oxides, such as PZT, has been essentially based on the wetting of the pore walls by the polymer-containing sols. However, successful growth of nanotubes of such oxides using electrophoresis seems to rely on the duplex structure of the alumina barrier layer formed on aluminum during anodization [23–26]. It has already been reported that this barrier layer consists of an n-type semiconductor alumina layer, at the electrolyte interface, and a dielectric passive layer at the Al electrode. By supplying the proper electrical path to the semiconducting layer, one should essentially be able to set the positively charged hydrolyzed metal species in the sol in motion and drive them toward the cathode [20, 21]. The changing resistance of the sol and the initial deposited layer as well as the different path lengths of electrical current in the semiconducting alumina can provide a basis for successful deposition of tubes in the template-based DC electrophoretic deposition.

X-ray diffraction analyses

X-ray diffraction (XRD) analyses were performed to evaluate both the composition and phase structure of the filled templates after firing. Because of the presence of carbon-containing precursors, a special firing schedule was used. The samples were soaked at about 350 °C for 30 min to ensure a complete burnout of the organic constituents. A steep heating rate (25 °C/min) was employed from 350 to 700 °C (final firing temperature) to minimize the formation of the intermediate phases [27]. The samples were then furnace cooled down to the room temperature in air.

Figure 9 represents the X-ray spectrum of a fired porous alumina template containing PZT nanotubes. The probable phases in this system include aluminum oxide, perovskite lead zirconate titanate or PZT, fluorite PZT, pyrochlore PZT, perovskite lead titanate or PT, perovskite lead zirconate or PZ, and some unreacted lead, zirconium and titanium oxides. All peaks were identified according to the JCPDS standard cards. The perovskite PZT phase was detected using card number 33-784. However, there is no standard X-ray diffraction file available for the fluorite or pyrochlore PZT. We have used the data supplied by Polli et al. [28] and Wilkinson et al. [29] to identify the fluorite PZT, and the d(hkl) values calculated by Wiedemann [30] to evaluate the presence of the pyrochlore PZT phase. It has already been reported that this calculation agrees well with both the X-ray data and transmission electron microscopy diffraction patterns [31]. The perovskite lead zirconate phase was detected by the JCPDS standard card number 3-655 and the formation of the lead titanate perovskite phase was evaluated using the standard card number of 2-804. Since the intensity of the lines due to the PZT phase was quite low, long data acquisition times of about 15 h were employed. The peaks in Fig. 9 indicate the presence of the perovskite PZT as the main phase, along

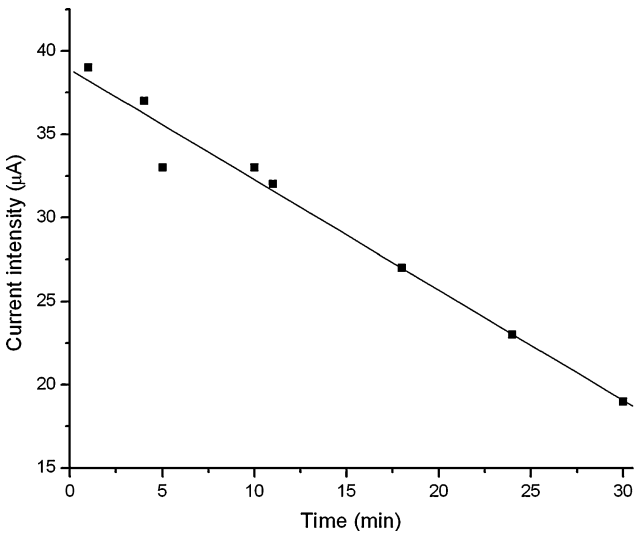

Fig. 8 Variation of the electrophoretic current versus time at the fixed applied voltage of 1.2 V

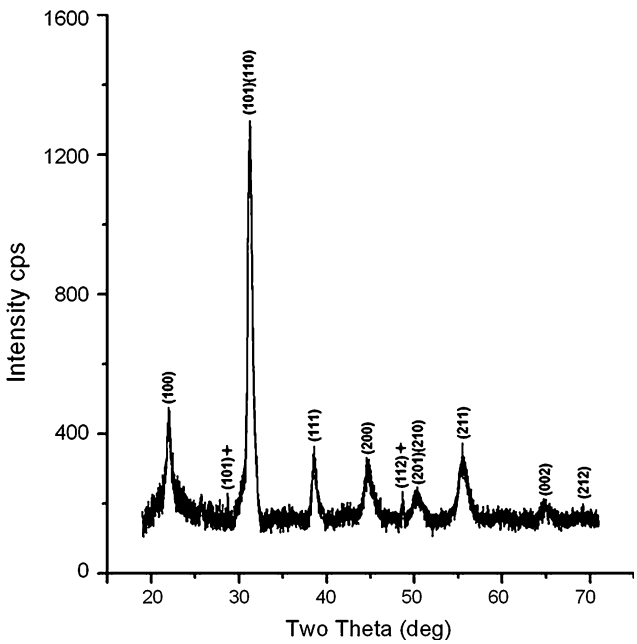

Fig. 9 XRD spectrum of an AA template containing PZT nanotubes. The marked peaks are due to PbO

with a small amount of lead oxide. No trace of crystalline Al_2O_3 in the XRD spectrum is expected since the porous anodic alumina is an amorphous material.

The absence of unreacted zirconium and titanium oxides indicates the good reactivity of the alkoxide precursors in the prepared PZT sol. However, the presence of unreacted lead oxide is due to the excess amount of lead in the initial composition. The excess lead is added to compensate for the lead loss, enhance crystallization of the amorphous PZT, and avoid formation of the fluorite (or pyrochlore) PZT phase upon firing. However, in the burnout stage, the carbonaceous species in the pyrolyzed amorphous PZT gel provide a local atmosphere which reduces the amorphous lead oxide to the elemental lead. This effect is known as Pb-partitioning and happens to varying degrees in samples containing excess lead [32]. Pb-partitioning causes the lead oxide to move out of the reaction and the remaining lead which is oxidized in the final firing (700 °C) does not re-enter into the reaction.

Conclusions

In this research, lead zirconate titanate nanotubes have been successfully grown through the template-based synthesis process, using homemade porous anodic alumina templates. The applicability of DC electrophoretic deposition for the production of tubular, rather rod or wire-like, PZT structure is demonstrated. We have shown the potential of this technique to obtain remarkable filling efficiency of the pores with the PZT precursor sol over a large area. By suitable choice of composition and firing process, perovskite PZT has been achieved as the main phase and the formation of undesirable non-ferroelectric phases is avoided. Flat and uniform arrays of parallel PZT nanotubes can then be produced by both ion-milling and etching of the template surface. The produced PZT nanotube arrays are good candidates for potential applications such as piezoelectric scanners, mass storage dynamic random access memories (DRAMs), and tunable photonic crystals.

Acknowledgements The authors thank Mrs. Gisela Baumann from "Solid Surfaces Analysis and Electron Microscopy Group" at Chemnitz University of Technology, for scanning electron microscopy experiments and also for her contribution in chemical processes.

References

1. Morrison FD, Luo Y, Szafraniak I, Nagarajan V, Wehrspohn RB, Steinhart M, Wendorff JH, Zakharov ND, Mishina ED, Vorotilov KA, Sigov AS, Nakabayashi S, Alexe M, Ramesh R, Scott JF (2003) Rev Adv Mater Sci 4:114
2. Luo Y, Szafraniak I, Zakharov ND, Nagarajan V, Steinhart M, Wehrspohn RB, Wendorff JH, Ramesh R, Alexe M (2003) Appl Phys Lett 83:440. doi:10.1063/1.1592013
3. Wei X, Vasiliev AL, Padture NP (2005) J Mater Res 20:2140. doi:10.1557/JMR.2005.0264
4. Zhao L, Steinhart M, Yu J, Goesele U (2006) J Mater Res 21:685. doi:10.1557/jmr.2006.0078
5. Jaffe B, Cook WR, Jaffe H (1971) Piezoelectric ceramics. Academic Press, London
6. Johansson A (2006) Template-based fabrication of nanostructured materials, Acta, Universitatis Upsaliensis. Uppsala University Press, Uppsala
7. Schwartz RW (1997) Chem Mater 9:2325. doi:10.1021/cm970286f
8. Steinhart M, Wehrspohn RB, Goesele U, Wendorff JH (2004) Angew Chem Int Ed 43:1334. doi:10.1002/anie.200300614
9. Limmer SJ, Seraji S, Forbess MJ, Wu Y, Chou TP, Nguyen C, Cao G (2001) Adv Mater 13:269. doi:10.1002/1521-4095(200108)13:16≤1269::AID-ADMA1269≥3.0.CO;2-S
10. Ohgai T, Hoffer X, Fabian A, Gravier L, Ansermet JP (2003) J Mater Chem 13:2530. doi:10.1039/b306581b
11. Meng G, Cao A, Cheng JY, Vijayaraghavan A, Jung YJ, Shima M, Ajayan PM (2005) J Appl Phys 97:064303. doi:10.1063/1.1846942
12. Yin AJ, Li J, Jian W, Bennett AJ, Xu JM (2001) Appl Phys Lett 79:1039. doi:10.1063/1.1389765
13. Lombardi I, Magagnin L, Cavallotti PL, Carraro C, Maboudian R (2006) Electrochem Solid-State Lett 9:D13. doi:10.1149/1.2181287
14. Zhao AW, Ye CH, Meng GW, Zhang LD, Ajayan PM (2003) J Mater Res 18:2318. doi:10.1557/JMR.2003.0325
15. Limmer SJ, Seraji S, Wu Y, Chou TP, Nguyen C, Cao G (2002) Adv Funct Mater 12:59. doi:10.1002/1616-3028(20020101)12:1≤59::AID-ADFM59≥3.0.CO;2-B
16. Limmer SJ, Cao G (2002) Adv Mater 15:427. doi:10.1002/adma.200390099
17. Cao G (2004) J Phys Chem B 108:19921. doi:10.1021/jp040492s
18. Jessensky O, Müller F, Gösele U (1998) Appl Phys Lett 72:1173. doi:10.1063/1.121004
19. Li AP, Müller F, Birner A, Nielsch K, Gösele U (1999) Adv Mater 11:483. doi:10.1002/(SICI)1521-4095(199904)11:6≤483::AID-ADMA483≥3.0.CO;2-I
20. Yi G, Sayer M (1996) J Sol–Gel Sci Technol 6:65. doi:10.1007/BF00402590
21. Yi G, Sayer M (1996) J Sol–Gel Sci Technol 6:75. doi:10.1007/BF00402591
22. Besra L, Liu M (2007) Prog Mater Sci 52:1. doi:10.1016/j.pmatsci.2006.07.001
23. McCafferty E (2003) Corros Sci 45:301. doi:10.1016/S0010-938X(02)00095-1
24. Guo QX, Hachiya Y, Tanaka T, Nishio M, Ogawa H (2006) J Lumin 119–120:253
25. Vrublevsky I, Parkoun V, Schreckenbach J, Goedel WA (2006) Appl Surf Sci 252:5100. doi:10.1016/j.apsusc.2005.07.028
26. Vrublevsky I, Jagminas A, Schreckenbach J, Goedel WA (2007) Appl Surf Sci 253:4680. doi:10.1016/j.apsusc.2006.10.038
27. Miller WD, Chapin LN, Evans Jr JT (1990) US patent no. 4,946,710
28. Polli AD, Lange FF, Levi CG (2000) J Am Ceram Soc 83:873
29. Wilkinson AP, Speck JS, Cheetham AK, Natarajan S, Thomas JM (1994) Chem Mater 6:750. doi:10.1021/cm00042a009
30. Wiedemann KE (1983) MS thesis, Virginia Polytechnic Institute & State University
31. Kwok CK, Desu SB (1992) Appl Phys Lett 60:1430. doi:10.1063/1.107312
32. Bel Hadj Tahar R, Bel Hadj Tahar N, Ben Salah A (2007) J Mater Sci 42:9801. doi:10.1007/s10853-007-1966-2